Eur. Phys. J. Special Topics **226**, 467–475 (2017)

DOI: 10.1140/epjst/e2016-60267-7

THE EUROPEAN PHYSICAL JOURNAL SPECIAL TOPICS

Regular Article

Periodic orbits and synchronous chaos in lasers unidirectionally coupled via saturable absorbers

Eusebius J. Doedel[1,a] and Carlos L. Pando L.[2,b]

[1] Department of Computer Science, Concordia University, 1455 boulevard de Maisonneuve O., Montréal, Québec H3G 1M8, Canada
[2] Instituto de Física, Benemérita Universidad Autónoma de Puebla, Apdo. Postal J-48, Puebla, Puebla 72570, Mexico

Received 12 September 2016 / Received in final form 30 November 2016
Published online 6 March 2017

Abstract. We study a model for two unidirectionally coupled molecular lasers with a saturable absorber. Our numerical bifurcation study shows the existence of isolas of in-phase periodic solutions as physical parameters change. There are also other non-isola in-phase and intermediate-phase families of periodic oscillations. The coupling parameter strongly affects the stability of these periodic solutions. In this model the unstable periodic orbits belonging to the in-phase isolas constitute a skeleton of the attractor, when chaotic synchronization sets in for a set of physically relevant control parameters.

1 Introduction

Synchronization is a special type of behavior in complex systems, and refers to a process in which rhythms of interacting entities are adjusted when they are properly coupled [1–3]. Generally the idea of synchronization gives a useful framework to study the collective behavior of coupled nonlinear systems. Review articles [1,2] provide an account of advances achieved in this multidisciplinary field, where many physical, chemical, biological, and ecological systems have been studied.

Chaotic synchronization (CS) may appear somewhat counterintuitive, since the sensitivity of the chaotic trajectories to small variations in the initial conditions seems incompatible with the long term convergence of trajectories that are sufficiently close initially. However, it has been demonstrated both theoretically and experimentally [4–9] that chaotic systems under suitable mutual interactions are capable of exhibiting different kinds of synchronization behavior. Several types of CS have been identified, such as complete synchronization, generalized synchronization, phase synchronization, lag synchronization, and anticipated synchronization [1,3]. More recent studies concentrate also on complex networks, which have a wide range of interdisciplinary applications ranging from neural networks to coupled lasers [2]. In many applications the transmission time between oscillators is larger than their intrinsic time scales.

[a] e-mail: doedel@cs.concordia.ca
[b] e-mail: carlos@ifuap.buap.mx

Thus, networks with time-delayed interactions are a focus of active research [10]. In particular, crowd synchrony and quorum sensing may occur when a large number of oscillators undergo delayed interactions with each other via a common information pool [11]. From the point of view of practical applications, another relevant issue is chaotic synchronization in multistable systems [12,13].

In the present study we consider a fundamental case: CS under unidirectional coupling, where the coupling is strongly nonlinear. In contrast, most coupling schemes that have been studied have used linear terms, as in earlier works [14–16], and later in the well-known articles of Pecora and Carroll [17,18]. Another feature of our work is that we base our study on a bifurcation analysis of relevant families of periodic orbits that explains the origin of CS. Another important characteristic of our study is that we consider the dynamics of a coupled optical system which can exhibit complex mixed mode oscillations. Mixed mode oscillations (MMO) display multiple time scales and are currently the subject of substantial research in several experimental systems [19–24]. Although our model can be generalized easily to networks of laser oscillators, we choose to study the basic master-slave configuration due to its already complex bifurcation structure for physically relevant parameters.

Laser devices in Q-switching operation typically emit short, intense pulses of light that are followed by time intervals with minimal laser intensity [25–27]. For this type of lasers, a saturable absorber element allows the energy inside the system to be accumulated and stored long enough before it is suddenly released as an optical pulse. These periodic pulses are an example of MMO. In this article we consider a special type of optical coupling for Q-switched lasers, namely, coupling via saturable absorbers. This coupling mechanism has been studied theoretically and experimentally for CO_2 lasers [28–30], where one of the main goals was precisely to achieve optical chaotic synchronization. Our numerical study of the bifurcations, and simulations using the model, allow us to explain qualitatively the origin of CS in these experiments.

We show that for a model of two unidirectionally absorber-coupled Q-switched CO_2 lasers there are isolas of in-phase periodic solutions. This model also shows characteristic families of in-phase and phase-locked periodic solutions. The former arise from Hopf bifurcations along families of stationary solutions. Periodic solutions having an intermediate-phase difference arise from subsequent symmetry-breaking bifurcations. The unstable periodic orbits (UPO) which arise from the in-phase isolas constitute the skeleton of the attractor when chaotic synchronization sets in. It is worthwhile mentioning that these isolas do not exist in the basic rate-equation model [31]. Our solutions are complemented by two-parameter bifurcation diagrams in the plane of the pump current and coupling strength, as obtained by a numerical continuation study with the package AUTO [32]. In Section 2 we introduce and discuss the model, and in Section 3 we present its bifurcation analysis and numerical simulations; conclusions and a discussion are presented in Section 4.

2 The model

We consider unidirectional coupling in class-B single-mode Q-switched lasers: a master-slave configuration for a pair of CO_2 lasers with a saturable absorber (LSA). Each of the uncoupled lasers is described by a model which is a reduced four-level LSA model [33,34]. The CO_2 LSA is an important example of class-B lasers and its giant laser spikes are known as passive Q-switching (PQS) self-pulsations, which are a good example of MMOs. The complex instabilities found in this system gave rise to early studies in nonlinear dynamics about three decades ago [25,27,35–38]. The rich dynamical phenomenology of the CO_2 LSA made it an interesting object for study in nonlinear dynamics [39–47]. We consider a special type of optical coupling

in Q-switched lasers, namely coupling via saturable absorbers, which is also a form of incoherent coupling. This coupling mechanism between laser devices has been implemented theoretically and experimentally in previous studies of CO_2 lasers [28–30].

Each of the two laser devices is described by a reduced four-level model [33,34] and the unidirectional coupling is via a fast saturable absorber. This system is modeled in equation (1), where I_i stands for the field intensities within the laser cavities, the fast variables, and v_i and w_i denote the effective populations of the lower and upper (excited) rotational energy levels in the gain medium, respectively, with $i = 1, 2$. Here v_i and w_i are the slow variables. Q is the incoherent pump induced by the excitation current in the gain medium, and z is the effective number of reservoir rotational levels in each vibrational band in the gain medium. The last term in the equations for I_i is for the saturable absorber, the parameter α is proportional to the density of absorber molecules and β is known as the saturability [33,34], while c is the coupling constant. The vibrational relaxation rates for the upper (excited) and lower vibrational levels in the CO_2 molecules are called γ_2 and γ_1, respectively. The relaxation constants γ_i have been suitably normalized in equation (1).

$$
\begin{aligned}
\frac{dI_1}{dt} &= I_1\Big(-1 + \frac{(z+1)\Omega_1}{z}(w_1 - v_1) - \frac{\alpha}{1+2\beta I_1}\Big)\ , \\
\frac{dv_1}{dt} &= \Omega_1 I_1(w_1 - v_1) - \gamma_1 v_1\ , \\
\frac{dw_1}{dt} &= \Omega_1 I_1(v_1 - w_1) - \gamma_2 w_1 + z\gamma_2 Q\ , \\
\frac{dI_2}{dt} &= I_2\Big(-1 + \frac{(z+1)\Omega_2}{z}(w_2 - v_2) - \frac{\alpha}{1+2\beta((1-c)I_2 + cI_1)}\Big)\ , \\
\frac{dv_2}{dt} &= \Omega_2 I_2(w_2 - v_2) - \gamma_1 v_2\ , \\
\frac{dw_2}{dt} &= \Omega_2 I_2(v_2 - w_2) - \gamma_2 w_2 + z\gamma_2 Q\ .
\end{aligned}
\tag{1}
$$

Also in equation (1), we have defined

$$
\Omega_i = \frac{z+1}{(z+1)^2 + 2zI_i/\gamma_R'}, \quad i = 1, 2,
$$

where γ_R' stands for the characteristic rotational relaxation rates of CO_2 molecules within the same vibrational band [33,34]. Physical processes similar to those that take place in the active medium may also occur in a saturable absorber of a gas cell, but the absorber may also have a different nature, such as in semiconductor saturable absorbers (SESAM) devices [48]. Our model is for the case of two unidirectionally coupled CO_2 lasers [29]. The saturable absorbers are assumed to be fast and identical in both lasers when coupling is zero. Moreover, both laser models have exactly the same parameters. The only element of possible asymmetry is the presence of the unidirectional coupling in the slave laser. When synchronous periodic or chaotic solutions occur in the system then the coupling term in the absorber vanishes in the slave laser.

The fixed parameter values are $\alpha = 0.75$, $\gamma_R' = 0.2205$, $\gamma_1 = 0.0252$, $\gamma_2 = 0.00315$, $z = 10$, and $\beta = 200$, while Q and the coupling strength c are used as continuation parameters. The synchronous (or in-phase) solutions, *i.e.*, solutions with $I_1(t) = I_2(t) = I(t)$, $v_1(t) = v_2(t) = v(t)$, and $w_1(t) = w_2(t) = w(t)$, correspond to the solutions of the single laser model, but their stability properties depend on c.

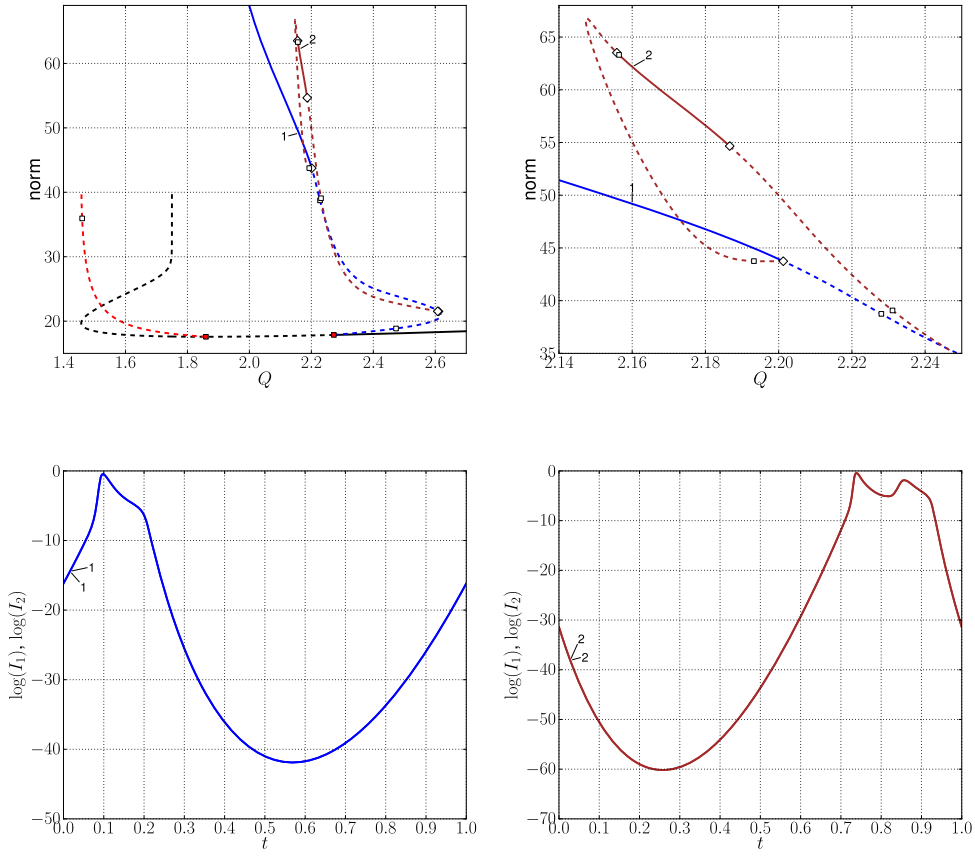

Fig. 1. The unidirectionally-coupled lasers for $c = 0.5$. Top-Left: A partial bifurcation diagram showing the L_2 norm (defined in the text) of the solutions versus Q. The black curve represents nonzero stationary states with two Hopf bifurcations (solid red squares), from which bifurcate a family of in-phase periodic solutions (blue), and a family of periodic solutions (red) along which the first laser is at rest. The brown family arises from the in-phase family via period-doubling bifurcations (open diamonds). There are also several branch points that lead to unstable families. Top-Right: A detail of the top-left panel. Bottom: Representative stable in-phase solutions at the points labeled 1 and 2 at in the top panels, showing $\log(I_1)$ and $\log(I_2)$ (which coincide) over one period, as a function of the scaled time variable t. The actual periods of these solutions are 515.113 and 720.695, repectively.

3 Numerical bifurcation analysis and synchronization

In this section we describe different families of solutions for equation (1). We do this for a value of the coupling constant c, namely, $c = 0.5$, where complete CS happens. The solution structure is significantly more complex than that of the single laser equations [33]. To develop insight into this structure, we explain it through a sequence of diagrams that together provide an overview of the basic solution families and their bifurcations. In our bifurcation diagrams, solid/dashed curves represent stable/unstable solutions, respectively, Hopf bifurcations are shown as solid red squares, branch points as small open squares, and period-doubling bifurcations as open diamonds.

Figure 1 presents a partial bifurcation diagram for $c = 0.5$, showing the norm of the solutions versus the pump parameter Q. Here the norm is simply the standard

vector L_2 norm for stationary states, and the integral L_2 norm for periodic solutions. The norm includes all six solution components, namely, $\log(I_i)$, v_i, w_i, $i = 1, 2$, while the integral is taken over the scaled time interval [0,1]. This particular representation is chosen mainly because of the clarity of the bifurcation diagrams that it produces. There are two Hopf bifurcations (HB) along the nontrivial stationary family, where $I_1 > 0$ and $I_2 > 0$. The blue curve represents the main family of in-phase periodic solutions that bifurcates from the HB on the right. The HB on the left does not lead to anti-phase orbits, as would be the case for mutually coupled laser oscillators [49], but rather to a family of periodic solutions along which the uncoupled (master) laser, I_1, is at rest. For the current value of the coupling constant c, namely $c = 0.5$, this family consists entirely of unstable solutions. However, it does contain stable regions when the value of the coupling constant c is small enough.

Concerning the basic in-phase family, Figure 1 shows that it contains a region of stable periodic orbits, namely to the left of a period-doubling bifurcation. Notice also the presence of branch points (open squares) along the in-phase family. In turn, the period-doubled family also has a region of stable solutions, bordered on the right by a secondary period-doubling bifurcation, and on the left by a branch point, with another period-doubling bifurcation closely nearby.

Figure 2 shows a more complete bifurcation diagram, again for the case $c = 0.5$, which also includes isolas of in-phase periodic solutions. The structure of these isolas is identical to that for the case of a single laser, but the stability properties are different, and depend on c. As seen in Figure 2, the isolas I_{03} through I_{07} contain stable regions for this value of c. These stable regions are bordered by period-doubling bifurcations, of which the one on the left is close to a fold, with a nearby branch point, as seen best in the top-right panel. Also notice the presence of branch points along the main in-phase family, along the period-doubled family, as well as further branch points along the isolas. The main folds and the main period-doubling bifurcations do not depend on the coupling constant c. However, the branch points do depend on c, and they are ultimately responsible for the disappearance of the stability regions. This loss of stability is clarified in Figure 3, where the top panels again show details of the bifurcation diagram in Figure 2, with $c = 0.5$. In particular, the top-left panel of Figure 3 shows part of the in-phase family (blue, labeled 1), the main period-doubled family (brown, labeled 2), and the isolas I_{03} to I_{12} (purple, labeled 3–12). The top-right panel provides a local view of the isolas I_{08} to I_{12}, which already do not have stable regions. As mentioned, the main folds and period-doubling bifurcations are independent of the coupling parameter c. This is evident in the bottom panel of Figure 3, which shows the loci of folds (black) and the loci of period-doubling bifurcations (blue) as perfectly vertical lines in the c versus Q diagram. However, the loci of branch points (red) do depend on c. In particular, none of the red curves reaches the bottom of the diagram, which means that the branch points gradually disappear as the coupling constant c decreases in value. Most of the stability regions seen in the top-left panel of Figure 3 are bordered by period-doubling bifurcations. However, as c decreases, branch points cross these period-doublings, and thereby become the new border of the stability region, as has already happened along the period-doubled family (brown, labeled 2) in the top-left panel of Figure 3. Ultimately, for small enough c, the branch points disappear, and with them the regions of stability.

It has been shown in physical experiments [28–30] that chaos synchronization of the characteristic PQS pulses is possible for suitable incoherent coupling via saturable absorbers. Our analysis indicates that this may happen for values of the pump (Q) slightly smaller than the HB of the in-phase family; where the HB is on the nontrivial stationary family. Figure 4 confirms this for $c = 0.5$, where panel (a) shows a time series for $\log(I_1)$. In panel (b) the autocorrelation function indicates the fast decay of correlations for the signal in (a), and panel (c) shows that complete synchronization

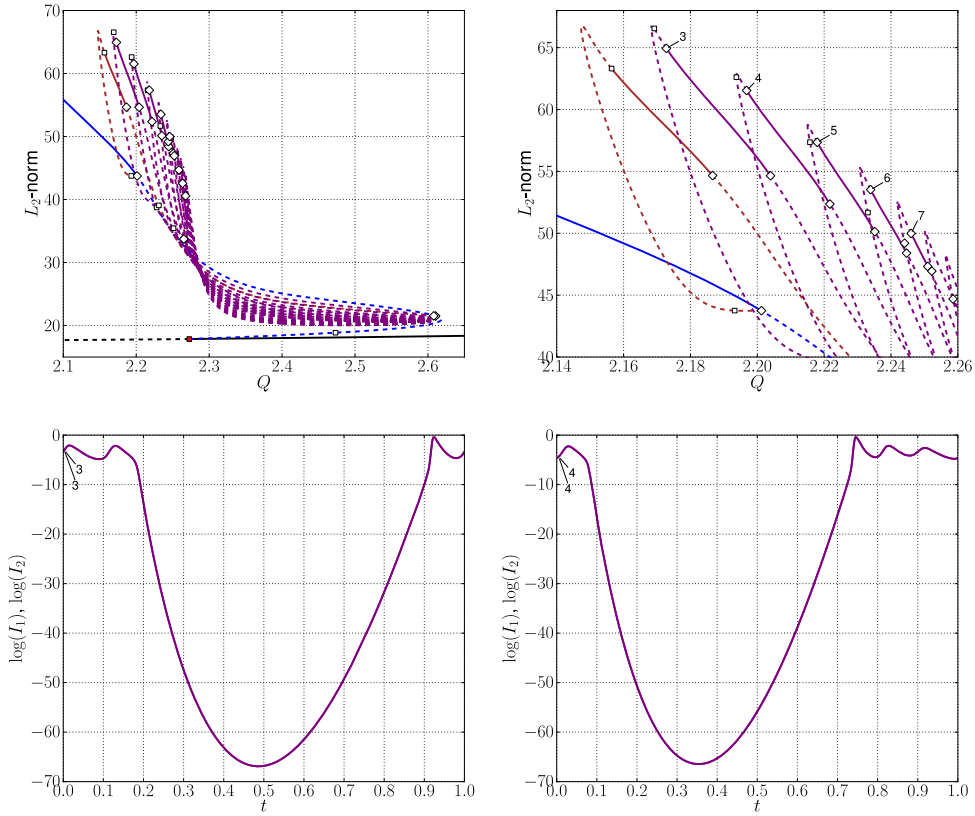

Fig. 2. The unidirectionally-coupled lasers for $c = 0.5$. Top-Left: Part of the bifurcation diagram in Figure 1, showing again the stationary family (black), the bifurcating in-phase family (blue) and its period-doubled family (brown), but now also showing the isolas I_{03} to I_{12} (purple). Top-Right: A detail of the top-left panel, showing in particular the isolas I_{03} to I_{07} (labeled $3-7$) more cleary; note that these contain stable regions. Bottom: Representative solutions (at period-doubling bifurcations) along the isolas I_{03} and I_{04}, showing $\log(I_1)$ and $\log(I_2)$ (which coincide) over one period, as a function of the scaled time variable t. The actual periods of these solutions are 833.191 and 896.828, repectively.

between the master and slave coupled lasers occurs. Finally, the histogram in panel (d) shows the probability for the neighborhoods of the UPOs on the in-phase isolas to be visited by the trajectory. This is in agreement with the existence of these UPOs in the bifurcation diagram for the pump Q in the top panels of Figure 3, which are blow-ups of top left panel in Figure 2 near $Q = 2.26$. For instance, for $Q = 2.26$ and $c = 0.5$ the trajectory cannot visit any UPO on isola I_{10} as its leftmost fold is to the right of $Q = 2.26$. In contrast, the UPOs of isolas I_n, $n = 4, 5, 6, 7, 8, 9$ are visited according to the histogram in Figure 4. Thus, the UPOs of the in-phase isolas constitute the skeleton of the attractor when complete chaotic synchronization of PQS sets in.

4 Conclusions and discussion

We have studied a rate-equation model of two unidirectionally coupled CO_2 lasers with a saturable absorber (LSA). For each uncoupled laser this model displays mixed-mode oscillations with one fast variable and two slow variables. In the bifurcation diagrams we show that the regions of stability of in-phase periodic orbits are generally bordered by period-doubling and symmetry-breaking bifurcations. The branch points

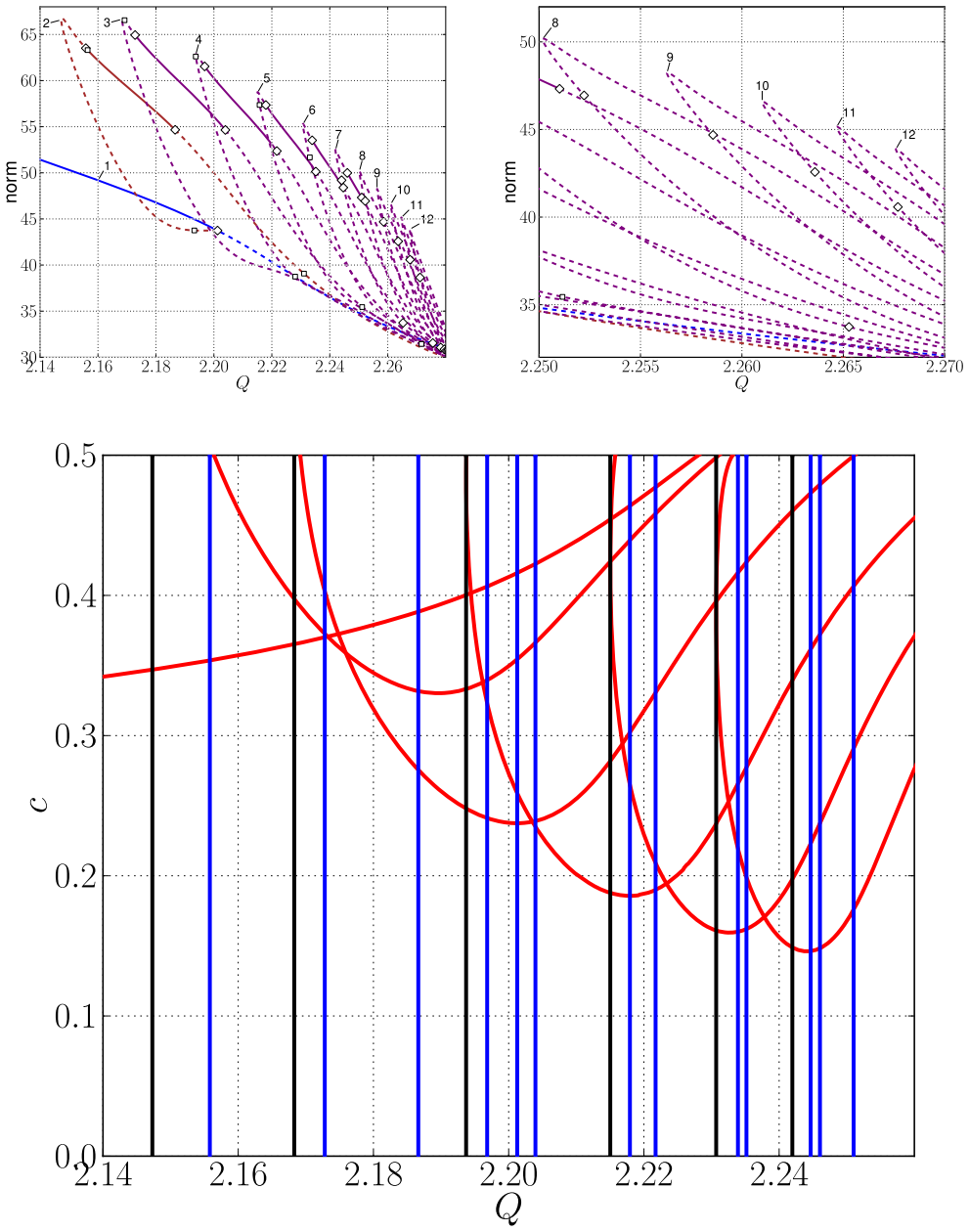

Fig. 3. The unidirectionally-coupled lasers for $c = 0.5$. Top-Left: A detail of Figure 2, showing the primary in-phase family (blue, labeled 1), the period-doubled family (brown, labeled 2), and the isolas I_{03} to I_{12} (purple, labeled 3-12). Top-Right: A detail of the top-left panel near $Q = 2.26$. Bottom: Loci of singular points, namely loci of folds (black), loci of period-doubling bifurcations (blue), and loci branch points (red). Note that the location of the folds and the period-doubling bifurcations does not depend on the coupling constant c. As explained in the text, the absence of red curves near the bottom of the diagram, *i.e.*, for small c, corresponds to the absence of regions of stability along the primary in-phase family, along the period-doubled family, and along the isolas.

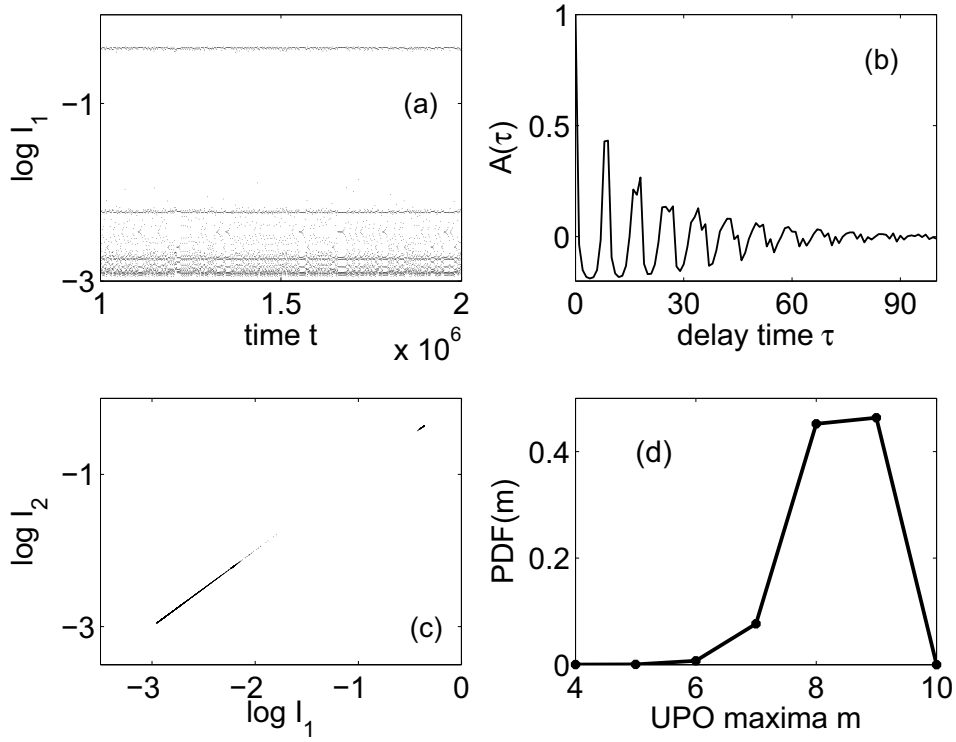

Fig. 4. (a) Time series for $\log(I_1)$ at the Poincaré section. (b) Autocorrelation function for the signal in (a) with delay time in units of the Poincaré section times. (c) Complete Chaotic synchronization between the lasers; $\log(I_1)$ versus $\log(I_2)$. (d) Histogram for the number of maxima m characterizing the neighborhoods of visited UPOs (see text). Coupling parameter $c = 0.5$ and $Q = 2.26$.

are strongly affected by the coupling parameter c, while the period-doublings are independent of c. In particular, for strong enough coupling, stable in-phase periodic passive Q-switching (PQS) pulses are possible. Similarly, when coupling is strong enough, complete chaotic synchronization may occur, where the attractor visits UPOs along families of in-phase isolas, *i.e.*, unstable PQS periodic pulses. Thus, we may conclude that the UPOs belonging to the in-phase isolas constitute the skeleton of the attractor when chaotic synchronization of PQS sets in.

This work was supported by NSERC (Canada), BUAP and CONACYT (México).

References

1. S. Boccaletti, J. Kurths, G. Osipov, D.L. Valladares, C.S. Zhou, Phys. Rep. **366**, 1 (2002)
2. S. Boccaletti, V. Latora, Y. Moreno, M. Chavez, D.U. Hwang, Phys. Rep. **424**, 175 (2006)
3. M. Rivera, G. Martinez Mekler, P. Parmananda, Chaos **16**, 037105 (2006)
4. S.K. Han, C. Kurrer, Y. Kuramoto, Phys. Rev. Lett. **75**, 3190 (1995)
5. M.A. Harrison, Y-Ch. Lai, R.D. Holt, Phys. Rev. E **63**, 051905 (2001)
6. K.S. Thornburg, Jr., M. Moller, R. Roy, T.W. Carr, R.D. Li, T. Erneux, Phys. Rev. E **55**, 3865 (1997)
7. P. Ashwin, J.R. Terry, K.S. Thornburg, Jr., R. Roy, Phys. Rev. E **58**, 7186 (1998)
8. C. Masoller, H.L.D. de S. Cavalcante, J.R. Rios Leite, Phys. Rev. E **64**, 037202 (2001)
9. I.Z. Kiss, V. Gaspar, J.L. Hudson, J. Phys. Chem. B **104**, 7554 (2000)

10. W. Just, A. Pelster, M. Schanz, E. Scholl, Phil. Trans. R. Soc. A **368**, 303 (2010)
11. J. Zamora-Munt, C. Masoller, J. Garcia-Ojalvo, R. Roy, Phys. Rev. Lett. **105**, 264101 (2010)
12. A.N. Pisarchik, R. Jaimes-Reategui, J.R. Villalobos-Salazar, J.H. Garcia-Lopez, S. Boccaletti, Phys. Rev. Lett. **96**, 244102 (2006)
13. A.N. Pisarchik, U. Feudel, Phys. Rep. **540**, 167 (2014)
14. T. Yamada, H. Fujisaka, Prog. Theor. Phys. **70**, 1240 (1983)
15. T. Yamada, H. Fujisaka, Prog. Theor. Phys. **72**, 885 (1984)
16. V.S. Afraimovich, N.N. Verichev, M.I. Rabinovich, Radiophys. Quantum Electron. **29**, 795 (1986)
17. L.M. Pecora, T.L. Carroll, Phys. Rev. Lett. **64**, 821 (1990)
18. L.M. Pecora, T.L. Carroll, Phys. Rev. A **44**, 2374 (1991)
19. M. Brons, T.J. Kaper, H.G. Rotstein, Chaos **18**, 015101 (2008)
20. M. Desroches, J. Guckenheimer, B. Krauskopf, Ch. Kuehn, H.M. Osinga, M. Wechselberger, SIAM Rev. **54**, 211 (2012)
21. J. Guckenheimer, C. Scheper, SIAM J. Appl. Dyn. Syst. **10**, 92 (2011)
22. J.G. Freire, J.A.C. Gallas, Phys. Lett. A **375**, 1097 (2011)
23. N. Baba, K. Krisher, Chaos **18**, 015103 (2008)
24. M. Desroches, B. Krauskopf, H.M. Osinga, Chaos **18**, 015107 (2008)
25. N.B. Abraham, P. Mandel, L.M. Narducci, in *Progress in Optics XXV*, edited by E. Wolf, (North-Holland, Amsterdam, 1988), pp. 1–190
26. T. Erneux, P. Glorieux, *Laser Dynamics* (Cambridge University Press, New York, 2010)
27. P. Mandel, *Theoretical Problems in Cavity Nonlinear Optics* (Cambridge University Press, New York, 2005)
28. A. Barsella, C. Lepers, D. Dangoisse, P. Glorieux, T. Erneux, Opt. Comm. **165**, 251 (1999)
29. T. Sugawara, M. Tachikawa, T. Tsukamoto, T. Shimizu, Phys. Rev. Lett. **72**, 3502 (1994)
30. I. Susa, T. Erneux, A. Barsella, C. Lepers, D. Dangoisse, P. Glorieux, Phys. Rev. A **63**, 013815 (2000)
31. E.J. Doedel, B. Krauskopf, C.L. Pando L., Eur. Phys. J. Special Topics **223**, 2847 (2014)
32. E.J. Doedel, B.E. Oldeman, et al., *AUTO-07P: Continuation and Bifurcation Software for Ordinary Differential Equations* (Concordia University, Montréal, 2011)
33. E.J. Doedel, B.E. Oldeman, C.L. Pando L., IJBC **21**, 305 (2011)
34. E.J. Doedel, C.L. Pando L., IJBC **22**, 1250238 (2012)
35. J. Dupré, F. Meyer C. Meyer, Rev. Phys. Appl. (Paris) **10**, 285 (1975)
36. E. Arimondo, F. Casagrande, L. Lugiato, P. Glorieux, Appl. Phys. B: Photophys. Laser Chem. **30**, 57 (1983)
37. M. Tachikawa, K. Tanii, M. Kajita, T. Shimizu, Appl. Phys. B: Photophys. Laser Chem. **39**, 83 (1986)
38. M. Tachikawa, K. Tanii, T. Shimizu, J. Opt. Soc. Am. B **4**, 387 (1987)
39. M. Tachikawa, F.L. Hong, K. Tanii, T. Shimizu, Phys. Rev. Lett. **60**, 2266 (1988)
40. M. Tachikawa, K. Tanii, T. Shimizu, J. Opt. Soc. Am. B **5**, 1077 (1988)
41. D. Hennequin, F. de Tomasi, B. Zambon, E. Arimondo, Phys. Rev. A **37**, 2243 (1988)
42. D. Dangoisse, A. Bekkali, F. Pappof, P. Glorieux, Europhys. Lett. **6**, 335 (1988)
43. M. Lefranc, D. Hennequin, D. Dangoisse, J. Opt. Soc. Am. B **8**, 239 (1991)
44. V.V. Nevdakh, O.L. Gaiko, L.N. Orlov, Opt. Comm. **127**, 303(1996)
45. L. de B. Oliveira-Neto, G.J.F.T. da Silva, A.Z. Khoury, J.R. Rios-Leite, Phys. Rev. A **54**, 3405 (1996)
46. P.C. de Oliveira, M.B. Danailov, Y. Liu, J.R. Rios-Leite, Phys. Rev. A **55**, 2463 (1997)
47. H.L.D. de S. Cavalcante J.R. Rios Leite, Chaos **18**, 023107 (2008)
48. U. Keller, Nature **424**, 831 (2003)
49. E.J. Doedel, C.L. Pando L., Eur. Phys. J. Special Topics **225**, 2613 (2016)